ELSEVIER

Sensors and Actuators B 26–27 (1995) 135–139

SENSORS AND ACTUATORS B CHEMICAL

Integrated array sensor for detecting organic solvents

J.W. Gardner [a,*], A. Pike [a], N.F. de Rooij [b], M. Koudelka-Hep [b], P.A. Clerc [b], A. Hierlemann [c], W. Göpel [c]

[a] *Centre for Nanotechnology and Microengineering, Department of Engineering, University of Warwick, Coventry CV4 7AL, UK*

[b] *Institute of Microtechnology, University of Neuchâtel, Rue A.-L. Breguet 2, CH-2000 Neuchâtel, Switzerland*

[c] *Center of Interface Analysis and Sensors, Institute of Physical and Theoretical Chemistry, University of Tübingen, Auf der Morgenstelle 8, D-72076 Tübingen, Germany*

Abstract

A new sensor array device has been designed to detect organic solvents; it comprises an array of six interdigital sensors lying upon a micromachined 0.5 μm thick silicon nitride membrane. There are three separate micromachined cells with two sensors per cell. In each cell, a thin film platinum resistance thermometer/heater is sandwiched in the middle of the silicon nitride layer in order to either monitor or control the temperature of the active layer. The array device has a low power consumption of $\approx$30 mW/sensor at 400 °C and is capable of operating at temperatures in excess of 600 °C, making it suitable for inorganic (e.g., SnO_2) as well as organic gas-sensitive materials. The sensor array device has been coated with both polymers and semiconducting oxides and its response to toluene, n-propanol and n-octane has been studied. The low power consumption and good thermal stability of this array device make it useful for application in portable gas monitoring equipment.

Keywords: Sensor arrays; Organic solvent detection; Silicon nitride

1. Introduction

There is considerable interest in the use of sensor array devices (SADs) in instruments both to analyse gas mixtures [1] and to recognise complex odours from foodstuffs and beverages [2]. A variety of sensing materials have been reported, but the two main classes are inorganic semiconducting oxides such as doped SnO_2 [3] and organic polymers that are conducting [4] or insulating [5]. The gas sensitivity of chemical sensors is, without exception, dependent on their operating temperature. Organic films have low melting points and so must be run at low temperatures, i.e., well below 100 °C for polymers. In contrast, semiconducting oxides are typically run at higher temperatures of between 300 and 500 °C, depending upon the target gas or gases. The fabrication of a ChemSAD that can operate adequately at high temperatures is not straightforward. Previous work on small planar devices has shown that a stable integrated heater can be difficult to achieve on silica, and that the power consumption of conventional devices made on silicon wafers is rather high at $\approx$1 W per sensor [6]. In this paper we report on the fabrication of an integrated sensor array device with an ultra-thin (500 nm) micromachined silicon nitride membrane. Such a device offers the possibility of low power consumption and thermal time constants, and stable temperature control at high operating temperatures. We report on the use of various coatings in order to detect organic solvents (e.g., n-octane).

2. Fabrication details

The devices were fabricated in a five-mask process of silicon wafers. The mask layouts were designed at Warwick University using the software package L-Edit (Tanner Research Inc., USA), and then sent to the electron beam lithography facility at the Rutherford Appleton Laboratory (Didcot, UK) for the preparation of the chrome photographic masks. The sensor array device consisted of three cells, each with an integrated platinum resistance thermometer/heater. Each cell contained two interdigital electrode pairs, making a total of 6 sensors per device. The silicon processing was carried out at the Institute of Microtechnology (Neuchâtel, Switzerland) as follows:

1. 80 nm of SiO_2 was thermally grown at 1100 °C on a 3-inch-diameter <100> silicon wafer (wafer thickness is 250 μm).

* Corresponding author.

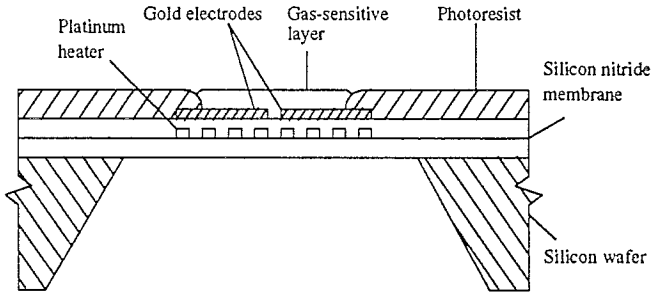

Fig. 1. Schematic cross section of one cell of the ChemSAD showing the ultra-thin silicon nitride membrane with an internal platinum resistance thermometer/heater.

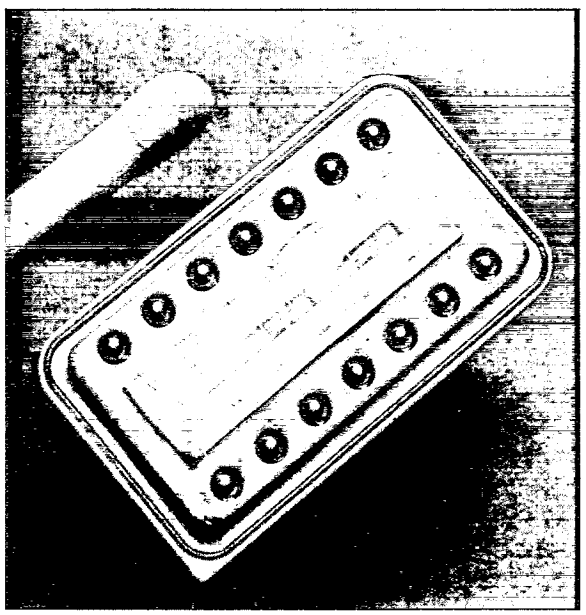

Fig. 2. Photograph of the sensor array device showing the three separate cells with a micromachined membrane, and wire-bonded onto a 14-pin d.i.l. header.

2. A 250 nm low-stress Si_3N_4 layer was deposited onto the wafer by low-pressure chemical-vapour deposition (LPCVD).
3. 200 nm of platinum was deposited (after a 10 nm tantalum seeding layer) and patterned with the first mask using a lift-off process to provide the resistance thermometer/heater.
4. A further 250 nm of Si_3N_4 was deposited by LPCVD to complete the membrane.
5. The Si_3N_4 was patterned with the second mask and plasma-etched to open up the platinum resistance thermometer/heater pads.
6. 300 nm of gold (after a 10 nm titanium seeding layer) was then deposited and patterned with the third mask to define both the sensor interdigital electrodes and sensor pads.
7. An anisotropic back-etch was carried out on the wafer patterned by mask five to realise the Si_3N_4 membranes and to provide snap-grooves [7].
8. A photoresist was finally spin-coated on the wafer as a passivation layer and patterned with mask four to open windows to the sensor electrodes and all pads. The windows in the passivation layer define the active area, and in the interdigital devices the entire heating area is exposed so that a high operating temperature can be used.

Fig. 1 shows a schematic diagram of the structure of a single cell. The interdigital electrodes have a separation of 10 μm and an aspect ratio of 210. The array chip is 16.2 mm by 4.25 mm and can be mounted on a standard 0.1-inch 14-way d.i.l. header, as shown in Fig. 2.

3. Materials deposition

Three different low-conduction polymers were dissolved in dichloromethane at room temperature, namely, polyethylcellulose, polycyanomethylsiloxane and polyurethane. The polymer coatings were then sprayed onto the silicon device with the deposition areas defined by aluminium masks. The coatings were cured at 60 °C for 48 h in air. Full experimental details have been reported elsewhere [8].

Three different suspensions of tin oxide (pure, 0.2% Pt, 0.2% Pd) were made up and a small drop pipetted onto each active area. The solvent was removed by placing the devices in an oven at 60 °C for 1 h. Then the thin oxide layers were annealed at 600 °C for 10 min in air to create a stable polycrystalline film.

Poly(pyrrole) tosylate was successfully grown on the substrates; the full technological details will be published later.

4. Results

4.1. Calibration of integrated platinum resistance thermometers/heaters

The platinum resistors were initially calibrated between 0 °C (ice-point) and 100 °C, as this is the operating range of most organic materials. The resistances were measured using a Keithley 175 multimeter while the device temperature was held constant ($\pm$0.1 °C) in a commercial heater (Techne Dri-Block DB-2P). Fig. 3 shows the temperature calibration curves of the platinum resistors for two SADs, i.e., six thermometers/heaters. The first device (SAD 1) demonstrates the typical values of the resistors of $\approx$190 Ω at 25 °C. The second device (SAD 2) shows somewhat lower values (down to 140 Ω) that were observed near the edges of the wafer. The platinum resistance–temperature data $R_H(T)$ were then fitted to the following equation in order to calculate

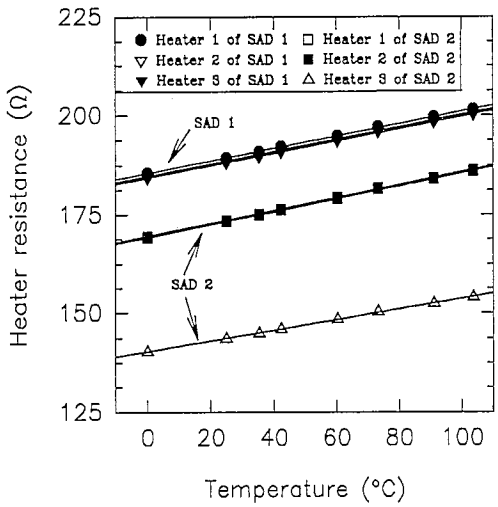

Fig. 3. Temperature calibration curves of the six integrated platinum resistors on two sensor array devices.

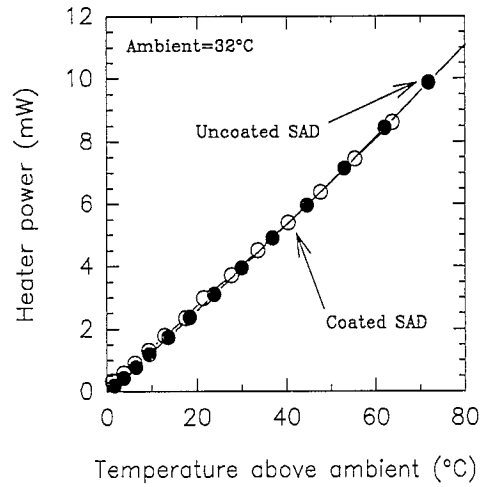

Fig. 4. Calibration of the heater power against cell temperature (relative to ambient) for a coated platinum resistor from SAD 1 and an uncoated platinum resistor from SAD 2.

Table 1
Temperature calibration parameters of integrated platinum resistors

SAD no.	Cell no.	R_0 (Ω)	α_0 (10^{-4}/°C)	ϵ (10^{-4})
1	1	185.6	8.34	5.6
1	2	184.4	8.33	5.0
1	3	184.8	8.36	7.4
2	1	140.4	9.47	6.4
2	2	169.7	9.56	7.5
2	3	169.3	9.60	6.9

the practical temperature parameters:

$$R_H(T) = R_0(1 + \alpha_0 T) \quad (1)$$

where R_0 is the resistance and α_0 is the temperature coefficient of resistance (TCR) of the platinum resistor at 0 °C, and T is the temperature in units of °C. The values for the six platinum resistors are given in Table 1. The TCRs of the platinum resistors were found to be $(8.9 \pm 0.7) \times 10^{-4}$/°C, which is somewhat lower than the value observed for pure platinum (38×10^{-4}/°C). The resistors behaved linearly, as expected, with the significance levels ϵ (1 − correlation coefficient) being better than 0.1%.

The platinum resistors were then calibrated to be heaters using a Knick DC-Calibrator J152 to provide a constant-current source and a Keithley 175 Multimeter to measure the voltage. Typical voltages required to obtain a cell temperature of 100 and 400 °C were 1.4 and 3.5 V, respectively. The exact voltage depends upon the heater resistance and thus process variability, but the power required to heat the cell is independent of the heater resistance or TCR, as shown by Fig. 4. The power consumption P_h of two platinum resistors has been plotted against its temperature above ambient, namely for heater 1 from SAD 1 and for heater 1 of

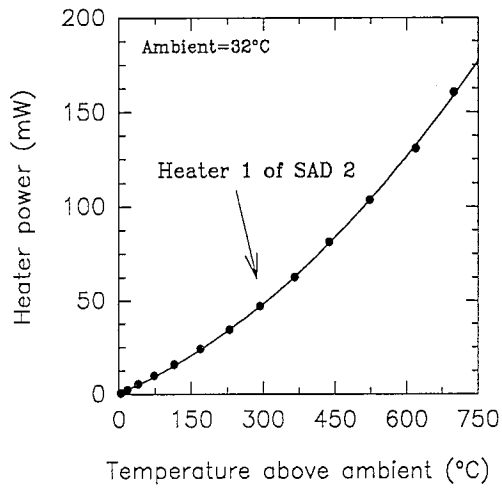

Fig. 5. Power required to heat a SAD device cell to a steady-state temperature.

SAD 2 (see Table 1). The calibration curves are linear, which indicates that the heat loss over this temperature range is dominated by thermal conduction through the substrate rather than by convection or radiation. As SAD 1 is coated with the polymers and SAD 2 is uncoated and the curves are colinear, we can surmise that heat conduction through the silicon nitride membrane is much greater than that through the thin polymer coatings. This is not surprising, as the polymers are both porous and paper-like. As shown by Fig. 5, the power loss becomes nonlinear at higher temperatures (above 150 °C) as thermal convection starts to be an important heat-loss mechanism. A good fit was observed of the data to the expected power law of

$$P_H = \alpha_p(T_H - T_{ambient}) + \beta_p(T_H - T_{ambient})^2 \quad (2)$$

The temperature coefficients of power, α_p and β_p, were calculated to be 1.1×10^{-1} mW/°C and 1.7×10^{-4} mW^2/°C from the data shown in Fig. 5. The heater resistance

was stable at temperatures of up to 700 °C, with some power loss by radiation.

4.2. Response to solvents

Fig. 6 shows the response of a tin oxide array device to 25 ppm and 50 ppm of n-octane in dry air at 30 °C, where each cell is held at 400 °C. The three plots show the typical response of each cell sensor with an observed change in resistance of 32.4% for the pure tin oxide, 16.3% for the Pd-doped and 26.1% for the Pt-doped. The response time of several minutes is determined by the flow injection system and not by the oxide sensors. The true rise and decay time constants have been measured to be typically 40 and 60 s, respectively, for toluene, n-propanol, methanol and n-octane. It was observed that there was a very high sensitivity to organic solvents at the ppm level, and the stability improved at 425 °C at 50% relative humidity, as shown in Fig. 7. 100, 100 and 50 ppm of toluene were measured with a background interference of 50, 100 and 100 ppm of CO gas. Polymer coatings showed no response to CO in previous experiments.

The capacitance and conductance of the polymer coatings were measured using a Hewlett-Packard 4263A *LCR* meter. The typical sensor capacitance and conductance at 10 kHz were found to be 2.0 pF and 2 nS, respectively. The low capacitance and conductance resulted in a high level of noise in the sensor signals, with a poor sensitivity to the organic vapours. The polymer resistivity is typically 10^{14} Ω cm, which makes it a very poor conductor. It is therefore necessary to increase still further the aspect ratio of the interdigitated electrodes or reduce the noise in the measuring setup. This problem, of course, does not occur with a conducting polymer (e.g., pyrroles) that has been grown successfully on the substrate and has a response of 0.1–10% to organic volatiles [9].

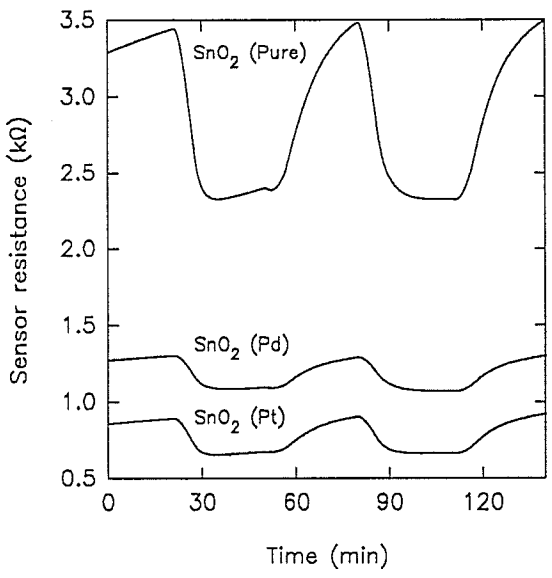

Fig. 6. Response of tin oxide films in an array device to 25 ppm and 50 ppm of n-octane in dry air.

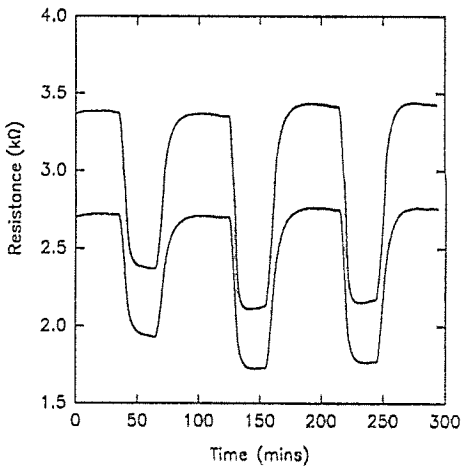

Fig. 7. Response of pure tin oxide to a mixture of toluene and CO in air at 50% relative humidity.

5. Conclusions

We report on the fabrication of an integrated sensor array device suitable for use with chemically sensitive coatings. The active areas can be run at a high operating temperature (400–600 °C), making it suitable for inorganic as well as organic materials.

Acknowledgements

We wish to thank Karl Bodenhöfer (University of Tübingen) for his help in measuring the organic volatiles, and Nicolae Barsan (Institute of Physics, Bucharest) for the tin oxide layers. One of us (J.W.G.) wishes to thank the Alexander von Humboldt Foundation for their financial support of his fellowship in Germany.

References

[1] S. Moore, J.W. Gardner, E.L. Hines, W. Goepel and U. Weimar, A modified multilayer perceptron model for gas mixture analysis, *Sensors and Actuators B, 15–16* (1993) 344–348.

[2] J.W. Gardner and P.N. Bartlett, A brief history of electronic noses, *Sensors and Actuators B, 18–19* (1994) 211–220.

[3] K. Ihokura and J. Watson, *The Stannic Oxide Gas Sensor*, CRC Press, Boca Raton, FL, 1994, 187 pp.

[4] P.N. Bartlett, P.B.M. Archer and S. Ling-Chung, Conducting polymer gas sensors. Part 1: Fabrication and characterisation, *Sensors and Actuators, 19* (1989) 125–140.

[5] K.D. Schierbaum, A. Hierlemann and W. Göpel, Modified polymers for reliable detection of organic solvents, *Sensors and Actuators B, 18–19* (1994) 448–452; *Synth. Met., 61* (1993) 37.

[6] P. Corcoran, H.V. Shurmer and J.W. Gardner, Integrated tin oxide sensors of low power consumption for use in gas and odour detection, *Sensors and Actuators B, 15–16* (1993) 32–37.
[7] K.E. Bean, Anisotropic etching of silicon, *IEEE Trans. Electron Devices, ED-25* (1978) 1185–1193.
[8] A. Hierlemann, W. Göpel, J. Mitrovics, M. Schweizer-Berberich and U. Weimar, Polymer-based sensor arrays and multicomponent analysis for the detection of hazardous organic vapours in the environment, *Sensors and Actuators B, 26–27* (1995) 126–134.
[9] P.N. Bartlett and S.K. Ling-Chung, Conducting polymer gas sensors. Part III: Results for four different polymers and five different vapours, *Sensors and Actuators, 20* (1989) 287–292.